Erbium Incorporation and Optical Properties of Er^{3+} ions in APE Er:LiNbO$_3$ Waveguides

Pavel Čapek, Josef Schröfel,
Faculty of Electrical Engineering, Czech Technical University
Technická 2, 160 00 Praha 6, Czech Rep.
xcapekp@feld.cvut.cz

Anna Macková,
Nuclear Physics Institute of ASCR, Rez near Prague, 250 68, Czech Rep.

R. Groetzschel,
Institute of Ion Beam Physics and Material Analysis, Forschungzentrum Rossendorf, Dresden, Germany.

Volkmar Dierolf, Christian Sandmann,
Dept. of Physics, Lehigh University, Bethlehem, PA, USA

Pavla Nekvindová, Jarmila Špirková, Petr Macháč,
Institute of Chemical Technology, Technická 5, 166 28 Prague 6, Czech Rep.

We investigated the erbium incorporation in LiNbO$_3$ planar waveguides produced by annealed proton exchange using the RBS-channeling technique and site selective excitation-emission spectroscopy at low temperature. We found that, different from other methods of waveguide-production, the proton exchange has almost no influence on the incorporation and optical properties of the Er^{3+} ions.

Keywords: Er ions, proton exchange waveguides, site-selective spectroscopy, RBS-channeling

Introduction

Optical amplifiers and lasers based on rare earth dopants are important integrated optical devices with large application potential [1]. In recent years LiNbO$_3$ has emerged as one of the main host materials due to its very favorable electrooptical, acustoptical and non-linear properties. Moreover, several techniques have been established to create low loss optical waveguides. Among the rare earth ions Er^{3+} plays a prominent role due to its optical transition around 1.5 μm which makes it the active ion of choice for optical communication applications. Despite the well shielded character of the 4f electrons the optical transitions are influenced within a crystal by the presence of the other ions. Most notably the degeneracy of the states is removed leading in LiNbO$_3$ to a splitting in (2J+1)/2 Stark sublevels. Details of these splittings and the separation between states is determined by details of the local environment. It was found in several studies (e.g.: [2]) on bulk material that several different environments ("sites") are present in LiNbO$_3$, which are distinct by the way the required charge compensation is achieved.

An earlier systematic study [3] under application of external perturbations established an intuitive tool to connect spectral shifts in the optical transitions to changes in the nearest neighborhood and long range intrinsic electric fields and to distinguish between these two interaction types. These results make the Er^{3+} an ideal probe for the local environment and allow the study of interaction effects among dopants in LiNbO$_3$. While investigations on bulk material are abundant only few waveguide specific studies exist [4, 5, 6]. These are mainly limited to waveguides produced by Ti-diffusion and show that the Ti^{4+} ion strongly influence the local electric field experienced by the Er^{3+} while leaving the direct neighbor unchanged. The influence is manifested in the optical spectra by a significant inhomogeous broadening.

The proton exchange (PE) waveguides is another method for fabricating optical waveguides [7]. PE is based on a reaction of the lithium niobate wafer with a suitable acidic source

which results in a large increase of the extraordinary refractive index. The PE waveguides have high loss and degrade electro-optic properties. However, they can be substantially improved by the annealing of the waveguides. Properties of the resulting annealed proton exchange (APE) waveguides strongly depend on the exchange conditions as well as on any subsequent annealing conditions. One of the main advantages of APE waveguides is guiding only TM polarization or TE polarization for Z-cut $\langle 0001 \rangle$ or for X-cut $\langle 11\bar{2}0 \rangle$ of the $LiNbO_3$, respectively.

In this paper we extend our approach to APE waveguides and study how Er^{3+} ions are influenced in the this waveguide environment.

Sample preparation and experimental methods

The samples of $LiNbO_3$ used in this work were grown from the congruent melt to which our Er^{3+} dopant was added ($[Er^{3+}]$ = 500 ppm). The planar waveguides were fabricated by annealed proton exchange process at 213 ^{o}C for 3 hours. The waveguides were single mode for 1.5 μm and the proton profile reaches about 10 μm into the sample.

For comparision we used $LiNbO_3$ channel waveguides produced by Ti-diffusion (110 nm layer thickness, $T_{diff} = 1060^{o}C$, t = 10h) in the group of Prof. Sohler (University Paderborn, Germany). These waveguides were also designed to be single mode at 1.5 μm. The Er^{3+} doping levels in these samples were comparable to those of the bulk doped samples but the incorporation was achieved by indiffusion. For details see Ref. [8].

In order to study the lattice location of Er^{3+} we used the RBS (Rutherford Backscattering Spectrometry)-channeling technique which is based on the effect that channeling of energetic ion beam occurs when the beam is carefully aligned with a major symmetry direction of a single crystal. Channeled particles cannot get close enough to the atomic nuclei to undergo large angle Rutherford scattering - hence scattering from the substrate is drastically reduced by a factor of 100. Scattering kinematics separates the signal of the impurity Er^{3+} and host lattice of $LiNbO_3$. The angular yield curve is obtained by monitoring the yield of the impurity and the host lattice. From the angular yield curves (angular scans) of the axial channels in $LiNbO_3$ in 3 different directions (cuts) is possible to determine the Er^{3+} position in the measured cut and finally in the $LiNbO_3$ lattice [9]. In order to determine the lattice position of Er^{3+} in $LiNbO_3$ several relevant crystallographic directions have been selected to perform the angular scans. The angular scans along the X $\langle 11\bar{2}0 \rangle$, Y $\langle 01\bar{1}0 \rangle$, and Z $\langle 0001 \rangle$ axis were measured for the samples treated by APE X-cut, Y-cut and Z-cut. The RBS experiment was performed in the Forschungzentrum Rossendorf, Dresden (Germany) using a Van de Graaff accelerator. The beam of alpha particles 1.8 MeV was used.

Combined excitation-emission spectroscopy (CEES) is a very powerful tool to investigate subtle changes in the optical transitions to investigate the local energetical environment of erbium. It is described in detail in Ref. [5]. The CEES measurements were performed in the Lehigh University, Dept.Physics, PA, USA.

Experimental results and discussion

RBS. In the structure of $LiNbO_3$ four different lattice sites are available to be occupied by foreign ions: two substitutional octahedral sites (Li^+ and Nb^{5+}), an additional free octahedron and a tetrahedral vacancy sites. The scan along the $\langle 0001 \rangle$ axis is useful to disregard any position out from the z axis. The signal from Nb^{5+} ions is practically identical to that of Er^{3+} ions (see Fig. 1) and so it can be concluded that they are located in three possible positions along the z axis i.e. Nb^{5+} site, Li^+ site or structural octahedral site. For precise determination of Er^{3+} position inside the Li^+ octahedron we studied the scan along $\langle 01\bar{1}0 \rangle$ and $\langle 11\bar{2}0 \rangle$ axis (see Fig. 1). In the case of the octahedral position we should see the maximum in the scan along $\langle 11\bar{2}0 \rangle$ axis see [10], but we don't in our case. Finally, on the basis of computer simulations of
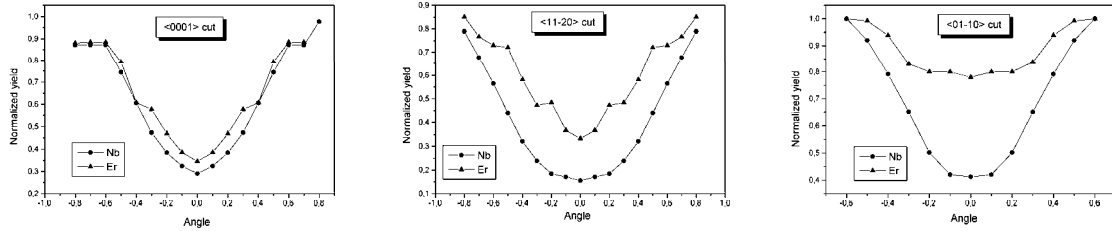
Fig. 1. LiNbO$_3$ angular scans along $\langle 0001 \rangle$, $\langle 01\bar{1}0 \rangle$ and $\langle 11\bar{2}0 \rangle$ axis.

the RBS data (Fig. 1) we can conclude that the Er^{3+} ion sites on the Li$^+$ site and is shifted in the direction along -z axis, similar as has been found for bulk material [10].

Excitation-Emission Spectroscopy. Inspecting the CEES data of the emission at around 550 nm obtained in the APE waveguides under excitation at around 450 nm and comparing it to bulk material and Ti:diffused waveguides reveals that the major sites are essentially unchanged. Subtle differences are found when individual emission spectra under identical excitation energies are compared for APE waveguide, the bulk and in the Ti-diffused waveguide. For instance, in the spectra shown in Fig. 2 three sites can be distinguished by decomposition. Earlier studies [2] showed that they all have the same primary charge compensation and are distinct in the secondary one. The sites, which are least perturbed (i.e. the secondary charge compensation is distant), exhibit in the depicted spectral range the emission peaks at the low energy side of the spectrum. Comparing first the APE waveguide and the bulk area we find a small tendency to the more perturbed sites, in which the secondary charge compensation or other perturbations are closer. Quite apparent is the absence of inhomogenous broadening (found in Ti-diffused waveguides) in the APE waveguides.

Although a quantitative interpretation of the difference between the perturbation induced by Ti and H require a more profound knowledge of the underlying defect configurations, a qualitative explanation is quite apparent. Both defects exchange for the Li$^+$ ion or occupy in congruent LiNbO$_3$ crystals the abundant Li-vacancies [11]. While H$^+$ requires on this site no charge compensation, the Ti^{4+} ion is quite "out of place" in terms of its charge and requires a complex compensation. This will result in changes in the electric field, which then are experienced by the Er^{3+} ion. These changes will increase as the Ti concentration increases and will hence lead to the observed inhomogenous linewidth. This phenomena is completely absent for H$^+$. The absence of any special new sites indicates that the H$^+$ ions - despite its charge neutrality - still seems to avoid the vicinity of the Er^{3+} ion. They only slightly perturb the more distant environment as indicated by the reduction of unperturbed sites.

The site-selectivity of the up-conversion excitation processes under 980 nm excitation have been investigated in bulk material and in Ti:LiNbO$_3$ waveguides. It was shown that two processes coexist in moderately Er^{3+} doped samples: (1) two-step excitation of a single Er^{3+} ion through two subsequent absorption processes and (2) up-conversion through a cross-relaxation process induced by energy transfer between two Er^{3+} ions within a cluster of ions. Choosing the emission energy appropriately the two processes and the involved defect sites can be distinguished. As expected from the barely changed site distribution, the up-conversion resembles the results obtained in bulk material. The most notable difference is a reduced overall up-conversion efficiency which can be explained by a reduction of the $^4I_{11/2}$ lifetime encountered in proton enriched samples due to the additional non-radiative decay channel into localized modes related with the hydrogen.
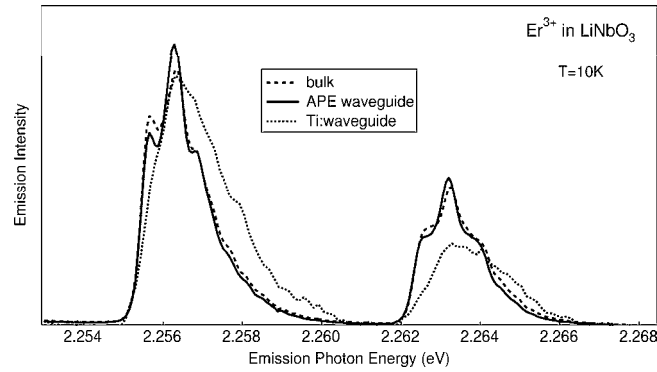
Fig. 2. Emission spectra (in the green spectral region) for two of the Stark-split transitions from the $^4S_{3/2}$ under excitation into the $^4F_{5/2}$ in the blue. Bulk doped Er^{3+}:LiNbO$_3$(dotted line), bulk doped Er^{3+}:LiNbO$_3$ with APE waveguide (solid), and Er^{3+}:LiNbO$_3$ Ti-diffusion waveguide (dashed).

Summary and conclusion

We investigated the incorporation and optical properties of Er^{3+} ions in lithium niobate waveguides produced by APE treatment. We found that the Er^{3+} ions occupy the Li^+ sites, just as in bulk LiNbO$_3$. No additional Er^{3+} sites appear, the distribution of sites is only slightly changed, showing a small reduction of the number of unperturbed defect sites, and in contrast to Ti-diffused waveguides, the spectral transitions exhibit no additional inhomogeous broadening.

In summary, it appears that the APE treatment leaves the environment of the Er ion almost unperturbed such that almost no waveguide specific properties could be observed.

[1] W. Sohler, H. Suche *Integrated Optical Circuits and Components: Design and Applications*, Marcel Dekker, New York, 127–159, 1999.

[2] V. Dierolf, M. Koerdt, *Phys. Rev. B* **61**(12), 8043–8052, 2000.

[3] V. Dierolf, A. Kutsenko, C. Sandmann, T. Tröster, G. Corradi, *J. of Lumin.* **87-89**, 989–992, 2000.

[4] B. Herreros, G. Lifante, F. Cusso, P. Townsend, P. Chandler, *J. of Lumin.* **72-74**, 198–200, 1997.

[5] V. Dierolf, A. Kutsenko, A. Ostendorf, W. von der Osten, W. Sohler, H. Suche, *Appl. Phys. B* **72**(7), 803–810, 2001.

[6] V. Dierolf, A. Kutsenko, A. Ostendorf, C. Sandmann, *Appl. Phys, B* **73**, 443–448, 2001.

[7] J. L. Jackel, C. E. Rice, J. J. Veselka, *Appl. Phys. Lett.* **41**(7), 607–608, 1982

[8] P. Becker, R. Brinkmann, M. Dinand, W. Sohler, H. Suche, *Appl. Phys. Lett.* **61**(11), 1257–1259, 1992.

[9] J. R. Tesmer, M. Nastasi, Contributing Editors J. Ch. Barbour, C. J. Maggiore, *Handbook of Modern Ion Beam Materials Analysis, Material Research Society*, Pittsburg, Pennsylvania, 1995

[10] L. Rebouta, P. J. ́ M. Smulders, D. o. Boerma, F. Agulló-Lopez, M. F. da Silva, J. C. Soares, *Phys. Rev. B* **48**(6), 3600–3610, 1993.

[11] T. Gog, M. Griebenow, T. Harasimowicz, G. Materlik, *Ferroelectrics* **153 (1-4)**, 249–254, 1994.